Superconducting properties and Hall effect of epitaxial NbN thin films

S. P. Chockalingam,[1] Madhavi Chand,[1] John Jesudasan,[1] Vikram Tripathi,[2] and Pratap Raychaudhuri[1,*]

[1]*Department of Condensed Matter Physics and Materials Science, Tata Institute of Fundamental Research,*
Homi Bhabha Road, Colaba, Mumbai 400005, India

[2]*Department of Theoretical Physics, Tata Institute of Fundamental Research, Homi Bhabha Road, Colaba, Mumbai 400005, India*

(Received 21 April 2008; published 4 June 2008)

We have measured the magnetotransport properties and Hall effect of a series of epitaxial NbN films grown on (100) oriented single crystalline MgO substrate under different conditions using reactive magnetron sputtering. Hall effect measurements reveal that the carrier density in NbN thin films is sensitive to the growth condition. The carrier density increases by a factor of 3 between the film with highest normal state resistivity ($\rho_n \sim 3.83$ $\mu\Omega$ m) and lowest transition temperature ($T_c \sim 9.99$ K) and the film with lowest normal state resistivity ($\rho_n \sim 0.94$ $\mu\Omega$ m) and highest transition temperature ($T_c \sim 16.11$ K), while the mobility of carriers does not change significantly. Our results show that T_c of NbN is governed primarily by the carrier density rather than disorder scattering. By varying the carrier concentration during growth, we can vary the effective disorder ($k_F l$) from the moderately clean limit to the dirty limit, which makes this system ideal to study the interplay of carrier density and disorder on the superconducting properties of an s-wave superconductor.

I. INTRODUCTION

Superconductivity in NbN thin films has been widely studied in the past decades motivated by diverse applications, such as Josephson junctions,[1] superconducting hot electron bolometers,[2] and superconducting single photon detectors.[3] Within conventional superconductors, NbN has high critical temperature ($T_c \sim 16$ K) combined with a short coherence length ($\xi < 5$ nm) and large penetration depth ($\lambda \sim 200$ nm), which allows fabrication of few nanometer thick superconducting thin films with moderately high T_c. In addition, NbN grows as epitaxial thin films on lattice matched substrates using popular thin film growth techniques, such as reactive magnetron sputtering[4–9] and pulsed laser deposition.[10,11] These films have good mechanical strength, are chemically stable in ambient atmosphere, and can be recycled from cryogenic temperatures to room temperature without any detectable degradation in their superconducting properties. Also, the existence of several other nitrides with widely varying properties, such as the ferromagnet GdN and the insulator AlN, opens the possibility of exploring fundamental issues, such as superconductor/ferromagnet proximity effect[12] and the role of interlayer coupling[13] on the superconducting properties of superconductor/insulator/superconductor multilayers.

Although there are several properties which are favorable for applications, T_c of NbN thin films is very sensitive to the growth conditions. Thin films with $T_c \sim 16$ K can only be synthesized under carefully optimized deposition parameters. Away from the optimal growth condition, T_c of the film decreases rapidly[4–11] to 10 K or below. It has been shown that there is a direct correlation between the normal state resistivity ρ_n and T_c (Ref. 5): Films with higher ρ_n have lower T_c. Such a direct correlation between ρ_n and T_c for an s-wave superconductor is not straightforward. While it is natural to attribute the increase in ρ_n to the increase in disorder in films grown away from the optimal condition, it was shown by Anderson[14] that scattering from nonmagnetic disorder is not expected to significantly affect T_c in an s-wave superconductor, as long as the system remains a metal.[15–17] On the other hand, ρ_n will also change if the carrier density is sensitive to the growth condition. In this case, the superconducting T_c, which is sensitive to the density of states [$N(0)$] at the Fermi level, is also expected to change. This possibility, which can be resolved through a determination of the carrier density through Hall effect in thin films with different T_c, has not been experimentally explored.

In this paper, we examine the role of carrier density and disorder on the superconducting properties of a series of epitaxial NbN films with T_c varying from 9.99 to 16.11 K. From measurements of the normal state and superconducting properties, we extract the key parameters, such as the carrier density (n), the Fermi wave vector (k_F), the mean free path (l), and coherence length (ξ_{GL}) for all the films. The central observation of this paper is that the carrier density (n) extracted from the Hall effect varies monotonically from $n \sim 6.47 \times 10^{28}$ e/m^3 in the film with the lowest T_c to $n \sim 1.98 \times 10^{29}$ e/m^3 in the film with the highest T_c. Analysis of the normal state and superconducting properties reveal that T_c of NbN films is governed primarily by the carrier density rather than disorder scattering. However, the disorder characterized by the Ioffe-Regel parameter,[18] $k_F l$, varies from the moderately clean limit ($k_F l \sim 7.15$) to the dirty limit ($k_F l \sim 2.56$), making this system ideal to look at the interplay between carrier density and disorder in an s-wave superconductor.

II. EXPERIMENTAL DETAILS

Thin films of NbN were synthesized through reactive dc magnetron sputtering by sputtering a Nb target in an Ar-N_2 gas mixture. The substrate temperature and ambient pressure during growth for all the films were fixed at 600 °C and 5 mTorr, respectively. Films with different T_c were synthesized using two different protocols. The first set of films (series 1) was synthesized by keeping the N_2/Ar ratio fixed at 20%

N_2–80% Ar, while the sputtering power on the Nb target was varied from 40 to 250 W. These films are named as 1-NbN-*x*, where *x* refers to the sputtering power, e.g., 40 for 40 W. The second set of films (series 2) was synthesized by keeping the sputtering power at 80 W and varying the N_2/Ar ratio from 10% N_2–90% Ar to 30% N_2–70% Ar. These films are named as 2-NbN-*y*, where *y* refers to the N_2 partial pressure, e.g., 30 for 30% N_2–70% Ar mixture. The thickness of all the films was larger than 50 nm to avoid the effect of epitaxial strain significantly affecting the structural and superconducting properties. The films were characterized through x-ray diffraction θ-2θ scans using Cu $K\alpha$ source. The epitaxial nature of the films was confirmed by performing ϕ scans around the [111] peak on a four-circle x-ray goniometer. The temperature dependence of resistivity $[\rho(T)]$ and T_c was measured through a conventional ac four-probe technique in a home built cryostat up to a maximum field of 5.8 T. The upper critical field was determined from $\rho(T)$-T scans in different applied magnetic fields (magnetic field perpendicular to the film plane) and determining T_c at various fields. To accurately determine $\rho(T)$, the electrical resistance was measured on a 1×10 mm^2 stripline deposited using a shadow mask. The thickness of the film was measured using an Ambios X P 2 Stylus profilometer at various positions on the stripline and the average value was taken as the film thickness. The thickness measured on different parts had a variation of $\sim$15%. However, since this figure is close to the resolution limit of our thickness measurements, this possibly does not reflect the intrinsic level of nonuniformity in the thickness. This is likely to be the biggest source of error in the calculation of resistivity and Hall coefficient. The Hall measurement was carried out using a four-probe ac technique. The Hall voltage was deduced from reversed field sweeps from +5.8 to −5.8 T after subtracting the resistive contribution.

III. RESULTS

Figures 1(a) and 1(b) show the representative x-ray diffraction θ-2θ scans for the films in both the series, plotted in logarithmic scale for the intensity. All the films other than 1-NbN-250 and 2-NbN-15 show a peak corresponding to the (200) peak of NbN, which crystallizes in the fcc structure. The end member of series 1 (1-NbN-250), namely, the film grown at the highest sputtering power, shows a prominent diffraction peak at 38.63° corresponding to the most intense peak (101) of Nb_2N with no peak corresponding to NbN. This is not unexpected since the effect of increasing the sputtering rate of Nb at a fixed N_2 partial pressure would increase the Nb/N ratio. Therefore, the stability of the NbN phase should be limited by a maximum power consistent with our observation. 2-NbN-15, on the other hand, shows only a very diffuse peak corresponding to NbN. For this film the superconducting transition is broad ($\Delta T_c \sim 2.5$ K) and the resistance below the transition temperature decreases to 0.1% of its value in the normal state but does not go to zero within our measurement resolution. We therefore do not consider this film in the rest of our analysis. For NbN films other than these two, we observe a very small amount of the Nb_2N impurity peak. We estimate the Nb_2N impurity phase to be
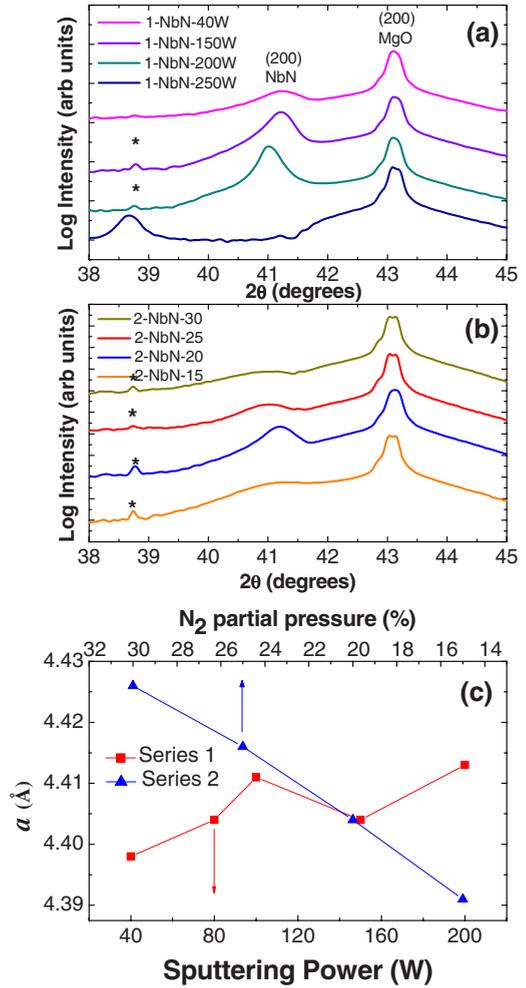
FIG. 1. (Color online) X-ray diffraction θ-2θ traces of epitaxial NbN films plotted in logarithmic scale for intensity: (a) series 1 and (b) series 2. Successive plots are shifted upward for clarity. All films other than 1-NbN-250 W show the (200) NbN peaks. The peaks marked $*$ correspond to Nb_2N impurity phase. (c) Lattice parameters as functions of sputtering power and N_2 partial pressure for NbN films in series 1 and series 2, respectively.

0.2–0.4 vol % of the NbN phase based on the ratio of the area under the peaks. The lattice parameters (a) of the NbN films calculated from the (200) peak are shown in Fig. 1(c). The epitaxy of all the films was confirmed from ϕ scan measurements on a four-circle x-ray goiniometer.

Figure 2(a) shows $\rho(T)$ vs. T for all the films. The normal state electrical resistivity (ρ_n) of the films measured at 17 K varies from 0.94 $\mu\Omega$ m for the least resistive film to 3.83 $\mu\Omega$ m for the most resistive film. T_c of the film is determined from the temperature at which the resistance falls to 10% of the normal state value. The inverse correlation between T_c and ρ_n is shown in Fig. 2(b). It is, however, instructive at this stage to look separately at ρ_n and T_c of the films [shown in Figs. 2(c) and 2(d)] in series 1 and series 2. For series 1, the NbN film with the smallest ρ_n and highest T_c forms close to the boundary between the Nb_2N and NbN phase. In series 2, T_c increases rapidly with increasing N_2 at low N_2 partial pressure followed by a gradual decrease at higher pressures. Our observation in series 2 is consistent
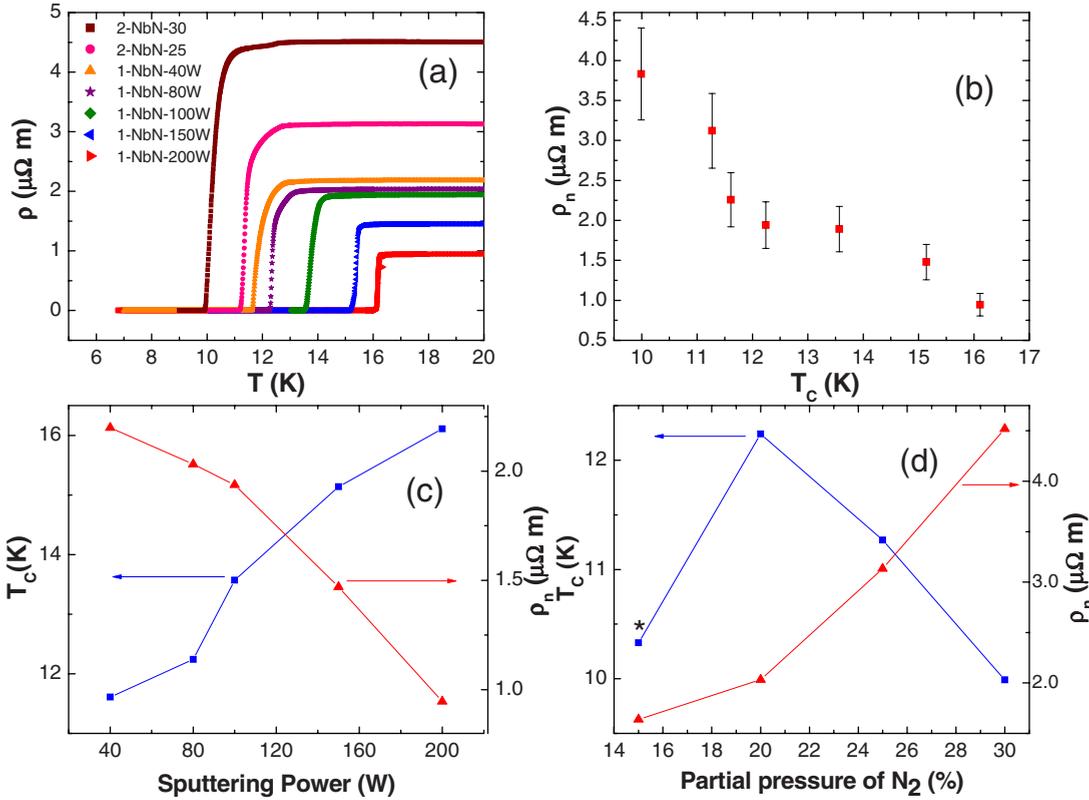
FIG. 2. (Color online) (a) Resistivity (ρ) as a function of temperature for all NbN films used in this study. (b) Normal state resistivity (ρ_n) measured at 17 K as a function of T_c. (c) ρ_n (▲) and T_c (■) as a function of sputtering power for NbN films in series 1. (d) ρ_n (▲) and T_c (■) as a function of N_2 partial pressure for NbN films in series 2; the sample 2-NbN-15 (marked as ∗) does not show zero resistance below the transition. The notional T_c is shown in panel (d) to indicate the overall trend in T_c with N_2 partial pressure.

with the N_2 partial pressure dependence of T_c reported by other groups.[5,6]

Figure 3 shows the Hall resistivity (ρ_{xy}) as a function of magnetic field for all the films measured at 17 K. The Hall coefficient ($R_H = \rho_{xy}/H$) is determined from the slope of the ρ_{xy}-H curve. It is interesting to note that the carrier density ($n = 1/R_H e$) extracted from R_H for the film with $T_c \sim 16.11$ K (1-NbN-200), $n = 1.97 \times 10^{29}$ e/m^3, is close to the theoretical estimate[19] of 2.39×10^{29} e/m^3. This agreement is remarkably good considering that the theoretical estimate was obtained by counting the number of electrons outside the closed shell of Nb under the assumption that the nitrogen atoms do not contribute. However, for films with lower T_c, n decreases significantly reaching a value $n = 6.47 \times 10^{28}$ e/m^3 for the films with $T_c \sim 9.99$ K (2-NbN-30).

Figure 4(a) shows the representative $\rho(T,H)$-T plots for the 1-NbN-200 films measured in different magnetic fields. $T_c(H)$ at different magnetic fields is determined from the temperature where $\rho(T)$ drops to 10% of the normal state value. The upper critical field (H_{c2}) as a function of temperature is plotted in Fig. 4(b) by inverting the $T_c(H)$ data for different films. The values of a, T_c, ρ_n, n, and $H_{c2}(T/T_c = 0.9)$ for all the films are listed in Table I.

IV. DISCUSSION

Table II lists the Fermi wave vector (k_F), the Fermi velocity (v_F), the electronic mean free path (l), the density of

states at the Fermi level [$N(0)$], the Ioffe-Regel parameter $k_F l$, the upper critical field at $T = 0$ [$H_{c2}(0)$], and the Ginzburg–Landau coherence length (ξ_{GL}) for all the films. k_F, v_F, l, and $N(0)$ are calculated from the free electron relations $k_F = (3\pi^2 n)^{1/3}$, $v_F = \hbar k_F/m$, $\rho = m/ne^2\tau = mv_F/ne^2 l$, and $N(0) = m/\hbar^2\pi^2(3\pi^2 n)^{1/3}$, where m is the mass of the electron and τ is the relaxation time. To check the reliability of the parameters obtained from the free electron relations,
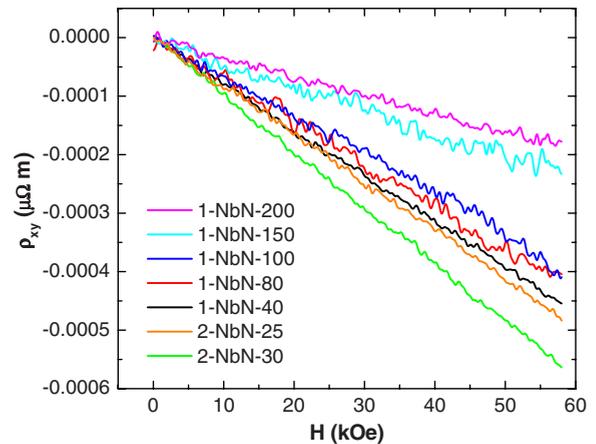
FIG. 3. (Color online) Hall resistivity ρ_{xy} as a function of H for all the films measured at 17 K. The Hall coefficient (R_H) is obtained from the slope of ρ_{xy}-H curve by fitting a straight line.
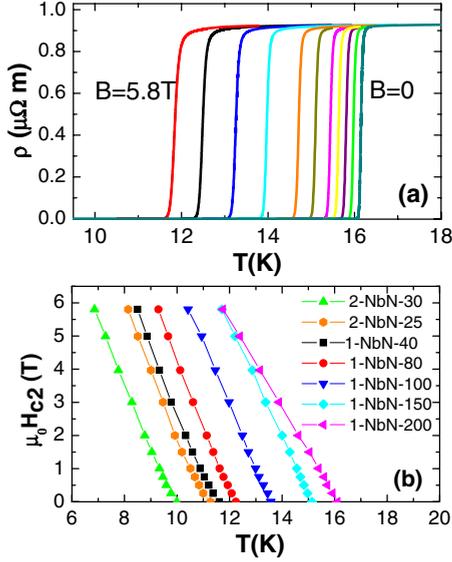
FIG. 4. (Color online) (a) Resistivity (ρ) as a function of temperature for 1-NbN-200 film in different applied magnetic fields. The successive magnetic field values are 0, 0.25, 0.5, 0.75, 1, 1.5, 2, 3, 4, 5, and 5.8 T. (b) The upper critical field (H_{c2}) as a function of temperature (T) for all NbN films.

we compare $N(0)$ with the value obtained from electronic structure calculations as well as specific heat measurements. Using the augmented plane wave method Mattheiss[20] calculated the density of states for stoichiometric NbN to be 0.54 states/NbN-eV. From specific heat measurements on NbN$_{1-x}$ single crystals, Geballe *et al.*[21] reported $N(0) \approx 0.5$ states/NbN-eV for the stoichiometric compound. For the film with $T_c = 16.1$ K, for which the n is closest to value expected for the stoichiometric compound, the carrier density obtained from our measurements corresponds to $N(0) \approx 0.515$ states/NbN-eV, which is in excellent agreement with these results. The consistency of $N(0)$ obtained using the free electron model may be traced back to the very short mean free path of the NbN films (3.96 Å for the film with $T_c \sim 16.1$ K). The presence of a large amount of disorder scattering is expected

to smear out any fine structure in the electronic density of states leaving only a free electronlike structure. This argument will hold even for the other films with lower T_c where the mean free path is shorter. Since all our films are in the dirty limit, $l \ll \xi_{GL}$, $H_{c2}(0)$ and ξ_{GL} are estimated from the dirty limit relation,[22]

$$H_{c2}(0) = 0.69 T_c \left. \frac{dH_{c2}}{dT} \right|_{T=T_c} \quad \text{and} \quad \xi_{GL} = [\Phi_0 / 2\pi H_{c2}(0)]^{1/2}.$$
(1)

Figure 5(a) shows the dependence of T_c on the carrier density n. T_c increases monotonically with increasing n. It is interesting to note that we do not see any correlation between T_c and the lattice parameter of the film when all the films are taken into account.[23] Figure 5(b) shows the variation of conductivity at 17 K, $\sigma_n (= 1/\rho_n)$, as a function of n. The conductivity follows a linear trend with $\sigma_n \propto n$, showing that the mobility of the carriers is not significantly different in different films.[24] The increase in ρ_n in films with lower T_c is therefore predominantly due to the decrease in carrier density rather than a change in scattering rate of the electrons. It therefore looks likely that T_c in different films is also primarily governed by the change in n rather than disorder scattering.

To understand the dependence of T_c on n beyond this qualitative picture, we analyze our data within the framework of McMillan theory[25] for strong coupling superconductors.[26] Within this theory, T_c is given by

$$T_c = \frac{\Theta}{1.45} \exp\left(-\frac{1.04(1+\lambda)}{\lambda - \mu^*(1+0.62\lambda)} \right),$$
(2a)

where λ is the electron-phonon coupling constant, μ^* accounts for the electron-electron repulsive interaction, and Θ is of the order of Debye temperature. Within McMillan theory, λ is proportional to the density of states at Fermi level $[N(0)]$,

TABLE I. Lattice parameter (a), superconducting transition temperature (T_c) normal state resistivity (ρ_n), electron density (n), and $H_{c2}(t = T/T_c = 0.9)$ for all the films in series 1 and series 2. Note that 1-NbN-80 and 2-NbN-20 correspond to the same film.

Sample	a (Å)	T_c (K)	ρ_n (17 K) ($\mu\Omega$ m)	n (e/m^3)	$\mu_0 H_{c2}$ at $T/T_c = 0.9$ (T)
1-NbN-200	4.4130	16.11	0.9459	1.97×10^{29}	2.16
1-NbN-150	4.4036	15.14	1.4787	1.61×10^{29}	2.59
1-NbN-100	4.4107	13.57	1.8914	9.28×10^{28}	2.54
1-NbN-80	4.4041	12.24	1.9401	8.72×10^{28}	2.22
1-NbN-40	4.3980	11.61	2.2575	8.00×10^{28}	1.77
2-NbN-15		10.73[a]			
2-NbN-25	4.4160	11.27	3.1203	7.60×10^{28}	1.59
2-NbN-30	4.4260	9.99	3.8311	6.46×10^{28}	1.59

[a]For this film the resistance decreases to 0.1% of its normal state value below the transition but does not go to zero. We list it here only to show the overall trend of T_c with N$_2$ partial pressure.

TABLE II. The Fermi wave vector (k_F), Fermi velocity (v_F), electronic mean free path (l), upper critical field [$H_{c2}(0)$], Ginzburg-Landau coherence length (ξ_{GL}), density of states at the Fermi level [$N(0)$], Ioffe–Regel parameter ($k_F l$), and electron-phonon coupling strength (λ) for all the films.

Sample	k_F (m^{-1})	v_F (m/s)	l (Å)	$\mu_0 H_{c2}(0)$ (T)	ξ_{GL} (nm)	$N(0)$ (states/m^3 eV)	$k_F l$	λ
1-NbN-200	1.80×10^{10}	2.09×10^6	3.96	14.80	4.72	2.38×10^{28}	7.15	1.64
1-NbN-150	1.68×10^{10}	1.95×10^6	2.91	17.82	4.30	2.23×10^{28}	4.90	1.53
1-NbN-100	1.40×10^{10}	1.62×10^6	3.28	17.58	4.33	1.86×10^{28}	4.60	1.28
1-NbN-80	1.37×10^{10}	1.59×10^6	3.34	16.65	4.45	1.82×10^{28}	4.58	1.25
1-NbN-40	1.33×10^{10}	1.54×10^6	3.04	15.12	4.67	1.77×10^{28}	4.05	1.21
2-NbN-25	1.31×10^{10}	1.52×10^6	2.28	14.79	4.72	1.74×10^{28}	2.98	1.19
2-NbN-30	1.24×10^{10}	1.44×10^6	2.07	13.08	5.02	1.65×10^{28}	2.56	1.13

$$\lambda = N(0) \frac{\langle g^2 \rangle}{M \langle \omega^2 \rangle} = K N(0), \tag{2b}$$

where $K = \langle g^2 \rangle / M \langle \omega^2 \rangle$, $\langle g^2 \rangle$ is an average over the square of the electron-phonon interaction matrix elements, $\langle \omega^2 \rangle$ is the average of the square of phonon frequency, and M is the mass of the ion. To fit our data to the McMillan equations, we rewrite Eqs. (2a) and (2b) as

$$\ln(T_c) = \ln\left(\frac{\Theta}{1.45}\right) - \frac{1.04[1 + KN(0)]}{KN(0) - \mu^*[1 + 0.62KN(0)]}. \tag{3}$$

We fit the variation of $\ln(T_c)$ with the $N(0)$ using $\ln(\Theta/1.45)$ and K as fit parameters. While making this fit we assume that Θ and K are the same for all films. This assumption is justified since the lattice constants for different films do not vary by more than 0.34% across both the series and hence we do not expect the phonon spectrum and the electron-phonon interaction matrix elements to change significantly for different films. In transition metal compounds, the value of μ^* is taken to be $\mu^* = 0.13$.[25,27] Figure 6 shows the fit of our data with Eq. (3). Barring one point all the points fall very close to the fitted plot within the error bars. The extracted value, $\Theta \approx 174$ K, is in the same ballpark as the reported values of Debye temperature,[21,27–29] which vary in the range of 250–320 K.[30] The value of λ (listed in Table II) calculated from the best fit value of K varies between $\lambda = 1.13$ and 1.64 consistent with the strong coupling nature of NbN. These values are in qualitative agreement with the value $\lambda = 1.45$ obtained by Kihlstrom et al.[31] from tunneling data on a film with $T_c = 14$ K. Despite this agreement, there are some points of caution in the preceding analysis. First, it has been suggested by Maekawa et al.[32] that large disorder could cause a decrease in $N(0)$ from its free electron value due to the loss of effective screening. Though our samples with lower T_c have $k_F l$ in the range where this effect could manifest itself, we do not observe such an effect from our data either in the normal[33] or the superconducting state. Second, the value of μ^* has to be critically assessed for disordered superconductors. It was argued by Anderson et al.[17,34] that for large disorder, the loss of effective screening can result in an increase in μ^* by an amount of the order of $\mu^*/(k_F l)^2$. To explore this possibility, we have also fitted the

data assuming $\mu^* = 0.16$. While the value of Θ remains the same, the value of λ increases by about 10% which is well within the error that we expect from this fitting procedure.

We now focus our attention to $H_{c2}(0)$ for all the films. For dirty superconductors $H_{c2}(0)$ is related to T_c and $N(0)$ through the expression[22] (in SI units)

$$H_{c2}(0) = 0.69 T_c \frac{4 e k_B}{\pi} N(0) \rho_n. \tag{4}$$

Figure 7 shows the experimental values of $H_{c2}(0)$ along with the calculated values using Eq. (4) as a function of ρ_n. Despite qualitative similarities there are significant differences. The value of $H_{c2}(0)$ calculated using Eq. (4) is significantly smaller than the experimental value for all the films. In addition, the calculated value of $H_{c2}(0)$ increases with ρ_n above 2 $\mu\Omega$ m, whereas the experimental value actually decreases. One source of error in the calculated value could be the use of the free electron density of states for $N(0)$. This, however, seems unlikely since $N(0)$ is consistent with specific heat measurements. We would like to note that there could be several sources of error in the values of $H_{c2}(0)$
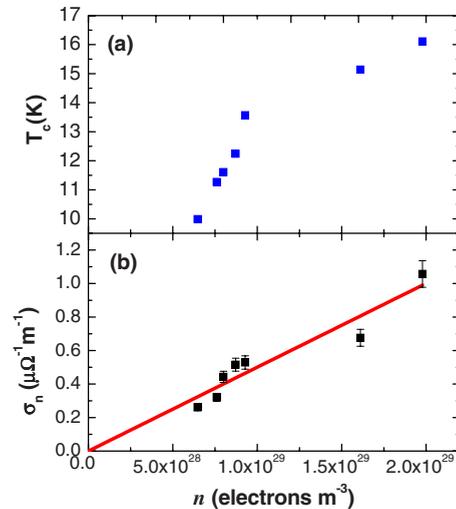
FIG. 5. (Color online) Variation of (a) T_c and (b) σ_n as a function of carrier density n. The straight line in (b) shows the linear fit to the data with the relation $\sigma_n = Kn$, where K is a constant.
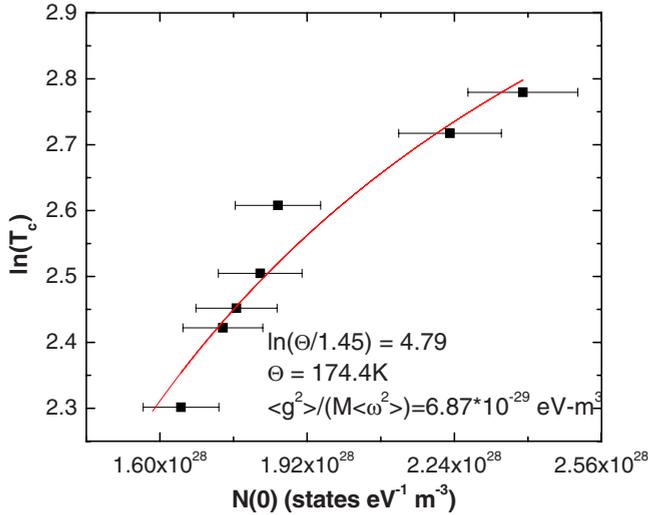
FIG. 6. (Color online) $\ln(T_c)$ as a function of the density of states at Fermi level, $N(0)$. The line shows a fit to the data with the McMillan theory for strong coupling superconductors.

FIG. 7. (Color online) Measured ($\blacktriangle$, $\bullet$) and calculated ($\blacksquare$) upper critical field [$H_{c2}(0)$] as a function of ρ_n. $\blacktriangle$ and $\bullet$ correspond to two different criteria used to determine $T_c(H)$.

extracted from Eq. (1). First, since the superconducting transition becomes broad in the presence of magnetic field, the experimental values of $T_c(H)$ depend very much on the criterion used to determine $T_c(H)$. To explore this possibility, we have also calculated $H_{c2}(0)$ by determining $T_c(H)$ from the value at which the resistivity is 50% of the normal state value (Fig. 7). While this changes the experimental values of $H_{c2}(0)$ by about 20% for films with higher ρ_n, the overall trend does not change significantly. Second, Eq. (1) is not universally valid. Significant deviation from Eq. (1) has been observed in dirty systems, where the critical field has been observed to increase linearly[35] with decreasing temperature down to 0.2 T_c. Also spin-orbit interactions can cause significant enhancement of $H_{c2}(0)$ over the value[22] given by Eq. (4). However, we believe that a more direct measurement of the critical field down to low temperatures at high fields is necessary to reliably address this issue.

We can try to speculate the reason behind the large change in carrier density on the deposition conditions in NbN. Since these films are grown by changing the sputtering power or N_2 partial pressure, it is expected that they differ in their Nb/N ratio. Previous studies on the dependence of electronic properties of NbN on stoichiometry were carried out on single crystals with nitrogen[21] vacancies. While we were unable to quantitatively determine the Nb/N ratio in these films using conventional techniques, nitrogen vacancies alone cannot explain our results. In series 1, the film with the highest $T_c \sim 16.11$ K forms close to the phase boundary between the Nb_2N and NbN phases. Since this film has a carrier density which is close to the expected value for the stoichiometric compound, it seems likely that this film has stoichiometry close to the Nb:N ratio of 1:1. In this series n (and T_c) decreases when we decrease the sputtering power. Since decreasing the sputtering rate of Nb decreases the Nb:N_2 ratio in the plasma, films grown at lower sputtering power should have lower Nb content. Therefore, films with lower n and T_c are likely to have Nb vacancies. (Similar argument will also
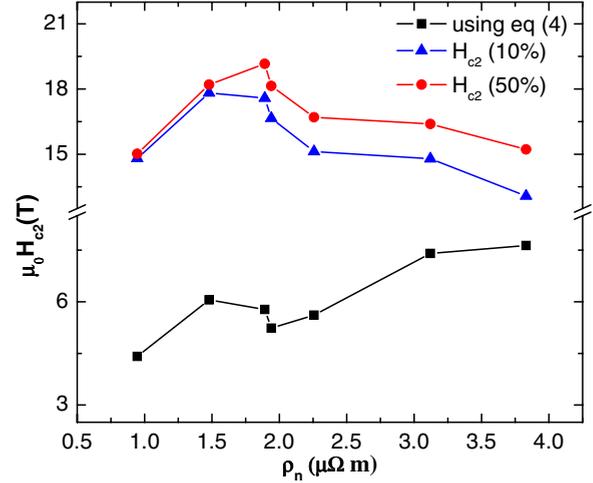
hold for series 2 where an increase in N_2 partial pressure above 20% results in a decrease in n and T_c in the range where the NbN crystallographic phase is stable.) Since the conduction electrons in this material come primarily from the electrons outside the close shell of Nb, an increase in Nb vacancies in the films would cause a sharp decrease in n. However, to account for a threefold decrease in n, we would need a very large degree of Nb vacancies, which is possibly unacceptable from the structural point of view. Since N vacancies also reduce n and $N(0)$ in the substoichiometric compound,[36,37] it is possible that the drastic reduction of carrier density is caused by a combination of Nb and N vacancies.[38] In addition, we cannot rule out the possibility of nontrivial modifications of the band structure caused by the presence of both Nb and N vacancies. This will require detailed calculations of the electronic structure beyond the rigid band picture, in the presence of Nb and N vacancies. Such calculations do not exist at present and is beyond the scope of this paper.

Finally, we would like to note that the ability to control the carrier density in NbN thin films provides a unique opportunity to look at the interplay of carrier density and disorder in an s-wave superconductor without any external doping. It is interesting to note that the Ioffe-Regel parameter, $k_F l$, which is a measure of the mean free path in terms of the de Broglie wavelength of the electron at the Fermi level, varies from 2.56 to 7.14. Since $k_F l \sim 1$ corresponds to the Mott limit for metallic conductivity, the level of disorder varies from moderately clean to the dirty limit. This provides an opportunity to look at the role of dynamic fluctuations as a function of disorder, as well as to probe recent theoretical predictions[15] of the formations of pseudogap state where the weak disorder limit breaks down. At least one such study has already been attempted[39] and we believe that our work will provide a much better understanding of those data. Our own investigations in this direction are currently underway and will be reported elsewhere.

V. CONCLUSION

We have explored the interplay of carrier density and disorder in epitaxial NbN films grown using dc magnetron sputtering. Our results show that T_c in these films is primarily governed by the carrier density which increases by a factor of 3 as we go from the film with the lowest $T_c \sim 9.99$ K to the films with the highest $T_c \sim 16.11$ K. By fitting our data with the McMillan theory, we obtain the value of the electron-phonon coupling parameter $\lambda \sim 1.07 - 1.55$, consis-

tent with the expected value for strong coupling superconductors.

*pratap@tifr.res.in

[1] J. C. Villegier, L. Viewx-Rochaz, M. Goniche, P. Renard, and M. Vabre, IEEE Trans. Magn. **21**, 498 (1985); A. Kawakami, Y. Uzawa, and Z. Wang, Appl. Phys. Lett. **83**, 3954 (2003).

[2] S. Cherednichenko, V. Drakinskiy, J. Baubert, J.-M. Krieg, B. Voronov, G. Gol'tsman, and V. Desmaris, J. Appl. Phys. **101**, 124508 (2007); P. Khosropanah, J. R. Gao, W. M. Laauwen, M. Hajenius, and T. M. Klapwijk, Appl. Phys. Lett. **91**, 221111 (2007); J. J. A. Baselmans, A. Baryshev, S. F. Reker, M. Hajenius, J. R. Gao, T. M. Klapwijk, B. Voronov, and G. Gol'tsman, J. Appl. Phys. **100**, 084510 (2006).

[3] Shigehito Miki, Mikio Fujiwara, Masahide Sasaki, Burm Baek, Aaron J. Miller, Robert H. Hadfield, Sae Woo Nam, and Zhen Wang, Appl. Phys. Lett. **92**, 061116 (2008); M. Ejrnaes, R. Cristiano, O. Quaranta, S. Pagano, A. Gaggero, F. Mattioli, R. Leoni, B. Voronov, and G. Gol'tsman, *ibid.* **91**, 262509 (2007); W. Słysz, M. Węgrzecki, J. Bar, P. Grabiec, M. Górska, V. Zwiller, C. Latta, P. Bohi, I. Milostnaya, O. Minaeva, A. Antipov, O. Okunev, A. Korneev, K. Smirnov, B. Voronov, N. Kaurova, G. Gol'tsman, A. Pearlman, A. Cross, I. Komissarov, A. Verevkin, and R. Sobolewski, *ibid.* **88**, 261113 (2006).

[4] J. R. Gavaler, J. K. Hulm, M. A. Janocko, and C. K. Jones, J. Vac. Sci. Technol. **6**, 177 (1969).

[5] Zhen Wang, Akira Kawakami, Yoshinori Uzawa, and Bokuji Komiyama, J. Appl. Phys. **79**, 7837 (1996).

[6] D. D. Bacon, A. T. English, S. Nakahara, F. G. Peters, H. Schreiber, W. R. Sinclair, and R. B. Van Dover, J. Appl. Phys. **54**, 6509 (1983).

[7] D. W. Capone II, K. E. Gray, and R. T. Kampwirth, J. Appl. Phys. **65**, 258 (1989).

[8] H.-J. Hedbabny and H. Rogalia, J. Appl. Phys. **63**, 2086 (1988).

[9] Y. M. Shy, L. E. Toth, and R. Somasundaram, J. Appl. Phys. **44**, 5539 (1973).

[10] R. E. Treece, M. S. Osofsky, E. F. Skelton, Syed B. Qadri, J. S. Horwitz, and D. B. Chrisey, Phys. Rev. B **51**, 9356 (1995); R. E. Treece, J. S. Horwitz, J. H. Classen, and Douglas B. Chrsey, Appl. Phys. Lett. **65**, 2860 (1994).

[11] K. Senapati, N. K. Pandey, Rupali Nagar, and R. C. Budhani, Phys. Rev. B **74**, 104514 (2006).

[12] J. Q. Xiao and C. L. Chien, Phys. Rev. Lett. **76**, 1727 (1996).

[13] E. S. Sadki, Z. H. Barber, S. J. Lloyd, M. G. Blamire, and A. M. Campbell, Phys. Rev. Lett. **85**, 4168 (2000).

[14] P. W. Anderson, J. Phys. Chem. Solids **11**, 26 (1959).

[15] The notion that disorder does not affect T_c in s-wave supercon-

ductors has recently been questioned. For details, see Y. Dubi, Y. Meir, and Y. Avishai, Nature (London) **449**, 876 (2007); A. Ghosal, M. Randeria, and N. Trivedi, Phys. Rev. Lett. **81**, 3940 (1998).

[16] Very close to the limit of Mott minimum metallic conductivity T_c can decrease because of the increase in electron-electron repulsion caused by the loss of effective screening (see Ref. 17).

[17] P. W. Anderson, K. A. Muttalib, and T. V. Ramakrishnan, Phys. Rev. B **28**, 117 (1983).

[18] A. F. Ioffe and A. R. Regel, Prog. Semicond. **4**, 237 (1960).

[19] M. P. Mathur, D. W. Deis, and J. R. Gavaler, J. Appl. Phys. **43**, 3158 (1972).

[20] L. F. Mattheiss, Phys. Rev. B **5**, 315 (1972).

[21] T. H. Geballe, B. T. Matthias, J. P. Remeika, A. M. Clogston, V. B. Compton, J. P. Maita, and H. J. Wiliams, Physics (Long Island City, N.Y.) **2**, 293 (1966).

[22] N. R. Werthamer, E. Helfland, and P. C. Honenberg, Phys. Rev. **147**, 295 (1966).

[23] For series 2, our variation of T_c with lattice parameters is similar to the one reported by Wang *et al.* (Ref. 5).

[24] The situation here is similar to heavily doped semiconductors where the mobility becomes independent of doping concentration. See S. C. Choo, M. S. Leong, and L. S. Tan, Solid-State Electron. **24**, 557 (1981).

[25] W. L. McMillan, Phys. Rev. **167**, 331 (1968).

[26] K. Komenou, T. Yamashita, and Y. Onodera, Phys. Lett. **28A**, 335 (1968).

[27] P. Roedhammer, E. Gmelin, W. Weber, and J. P. Remeika, Phys. Rev. B **15**, 711 (1977).

[28] Y. Pellan, G. Dousselin, J. Pinel, and Y. U. Sohn, J. Low Temp. Phys. **78**, 63 (1990).

[29] C. Geibel, H. Rietschel, A. Junod, M. Pelizzone, and J. Muller, J. Phys. F: Met. Phys. **15**, 405 (1985).

[30] We would like to note that Θ in McMillan theory arises from a phenomenological cutoff, which is of the order of the Debye temperature. A precise match between the two is therefore not expected.

[31] K. E. Kihlstrom, R. W. Simon, and S. A. Wolf, Phys. Rev. B **32**, 1843 (1985).

[32] S. Maekawa, H. Ebisawa, and H. Fukuyama, Prog. Theor. Phys. Suppl. **84**, 154 (1985).

[33] Since the loss of screening will affect $N(0)$ at the Fermi level but will have no effect on the carrier density n extracted from the Hall effect, the loss of screening should manifest itself as a

deviation from the linear trend in σ_n versus n at large disorder, which we do not observe in our data.

[34] The mechanism proposed by Anderson–Muttalib–Ramakrishnan (Ref. 17) has, however, been questioned by Leavens; see C. R. Leavens, Phys. Rev. B **31**, 6072 (1985).

[35] Sangita Bose, Pratap Raychaudhuri, Rajarshi Banerjee, and Pushan Ayyub, Phys. Rev. B **74**, 224502 (2006).

[36] P. Marksteiner, P. Weinberger, A. Neckel, R. Zeller, and P. H. Dederichs, Phys. Rev. B **33**, 6709 (1986).

[37] It is interesting to note that T_c decreases both for samples with excess Nb and excess N; E. K. Storms, A. L. Giorgi, and E. G. Szklarz, J. Phys. Chem. Solids **36**, 689 (1975).

[38] The situation here is possibly similar to the Ar ion irradiated NbN samples where the decrease in T_c after irradiation was attributed to the reduction in density of states caused by Nb or N vacancies; J. Y. Juang, D. A. Rudman, J. Talvacchio, and R. B. van Dover, Phys. Rev. B **38**, 2354 (1988).

[39] T. Ohashi, H. Kitano, A. Maeda, H. Akaike, and A. Fujimaki, Phys. Rev. B **73**, 174522 (2006).